JJEE
Volume X | Number X | Month 20XX | Pages XXX-XXX

Jordan Journal of Electrical Engineering

ISSN (print): 2409-9600, ISSN (online): 2409-9619

Homepage: jjee.ttu.edu.jo

Optimum Base Station Antenna Tilt Angle for Inter-Cell Interference Limited Mobile Cellular System

Araz S. Ameen[1*], Salah Y. Radhi[2]

[1] Electrical Engineering Department, University of Sulaimani, Sulaymaniyah, Kurdistan, Iraq
E-mail: araz.ameen@univsul.edu.iq
[2] Electrical Techniques Department, Sulaimani Technical Institute, Sulaimani Polytechnic University, Sulaymaniyah, Kurdistan, Iraq

Received: Oct 09, 2023 *Revised: Jan 20, 2024* *Accepted: Jan 29, 2024* *Available online: Jun 23, 2024*

***Abstract*—** This paper investigates the effect of base station (BS) antenna tilt angle on the performance of LTE-Advanced physical layer downlink channel in Inter-Cell Interference (ICI) limited scenario for five cell ranges, two carrier frequencies, and two BS antenna heights. The cellular system is deployed following the 3GPP hexagonal grid with a frequency reuse factor of one and three sectors per site. An urban based 3D ray-tracing tool is used to model the wireless channel for many BS and user equipment (UE) links. System performance is evaluated in terms of Signal power to Interference plus Noise power Ratio (SINR), received signal power, received interference power, achievable throughput (THR), Average Spectrum Efficiency (ASE) and UEs outage probability. The objective is to find the BS antenna tilt angle that provides the maximum ASE, minimum UEs outage probability, or optimum ASE and UE outage probability. The obtained simulation results unveil that the maximum ASE occurs at a tilt angle where the mean of the SINR is maximum and the mean of rms delay spread is minimum, while the minimum UEs outage occurs at a tilt angle where the received signal power is maximum. This is an important finding to facilitate the planning and the deployment of cellular system in the presence of ICI. Moreover it is found that the optimum tilt angles decrease as the cell range increase and BS antenna height decrease. The results also show that these optimum tilt angles are independent of the carrier frequency.

***Keywords*—** Antenna tilt angle; Average spectrum efficiency; Intercell interference; Outage probability; Interference plus noise power ratio.

1. INTRODUCTION

The global wireless communication standard traffic has been on a steady rise since the First Generation (1G) and continuous till now due to the growth in the capacity demand and Quality of Service (QoS). The evolution of the cellular mobile phone from the 1G analogue mobile phone systems to the Second Generation (2G) digital technology in the 1990 introduced new services such as Short Message Service (SMS) and download ringtones. Then the existence of the Third Generation (3G) became very important to achieve higher QoS for mobile subscribers set by the International Mobile Telecommunication (IMT)-2000 to fulfill the growing requirements towards mobile telecommunication technologies. Recently, rapid development is achieved in the wireless communications technologies in the Fourth Generation (4G) and the Fifth Generation (5G) to improve the performance of the cellular network and support a low latency reliable high data rate application for mobile users [1].

Due to the deficiency of spectrum resources the 4G and 5G standard deploy cellular systems with a frequency reuse factor of one to support high data rate application. This leads to the inevitable occurrence of Inter Cell Interference (ICI). ICI is an issue for mobile cellular

* Corresponding author
DOI: https://doi.org/10.5455/jjee.204-1696884748

networks that leads to degradation of the achievable Throughput (THR) performance at the Users Equipment (UE) as a result of the decrease in the received Signal power to Interference plus Noise power Ratio (SINR). In the cellular network, different parameters determine the level of ICI received power and SINR, such as frequency reuse factor, cell size, environment, Base station (BS) antenna height, and BS antenna down tilt angle [2]. BS antennas are vital components of any wireless system. The down tilt angle of the BS antenna is an important factor in cellular mobile network which used to improve the coverage and capacity of the networks depending on correct adjusting tilts, or inclination of the antenna in relation to an axis. Hence, the performance of cellular network can be improved by selecting appropriate BS antenna tilt angle. In addition, the height of the BS antenna is another important factor in determining the coverage of the BS and plays an important role for calculation of path losses in the channel [3].

Many studies are available in the literature to address the impact of the BS antenna tilt angle and other parameters on the performance of the cellular system. The study of [3] investigated the effects of high antenna heights, high gain antenna and downtilting in the frequency range (905 – 915) MHz at two existing cellular mobile radio sites. Their results showed that high gain sites, with high gain antennas and suitably selected pattern tilting, can be obtained by reducing both transmitted power from cell site and interfering sites.

A study for the impact of the mechanical antenna downtilt of the BS on the downlink capacity of a 6-sectored Wideband Code Division Multiple Access (WCDMA) cellular network is performed in [4] for site spacing of (2.2 km, 1.5 km) and BS antenna heights of (25 m, 40 m). The study of [4] showed that the capacity of the system depends on the mechanical downtilt angle and the reduction of the interference from other cells. In addition, their results showed that the handover areas are changed in accordance with the mechanical downtilt angle. It is also determined that the optimum tilt angle of the BS depends on the BS antenna height and site spacing. Both the capacity improvement and the optimum tilt angle increase as the site spacing decreases and BS antenna height increases. The study in [4] recommended a BS tilt angle of 12 degrees for a site spacing of 1.5 km when the BS antenna height is 40 m, and the elevation beamwidth is 12 degrees.

The authors in [5] studied the effect of repeaters and BS antenna tilt on the performance of WCDMA macro cellular network considering a carrier frequency of 2.1 GHz, a site spacing of 1200 m, and a BS antenna height of 32 m. They evaluated the impact of the optimum BS antenna tilt angle with or without repeaters. The results showed that the addition of repeaters improves the performance of the network considerably. Inclusion of repeaters requires an optimum BS antenna electrical downtilt angle of 9 degrees compared to 6 degrees in absence of repeaters.

A study is performed in [6] to investigate the impact of antenna downtilt on the performance of cellular WCDMA network. The study focuses on the impact of antenna downtilt on system capacity and network coverage. They found an optimum downtilt angle, which is defined by the site spacing, antenna height, and vertical beamwidth for various practical network configurations. Microcellular system is considered with site spacing of 1.5 km and 2.5 km, antenna height of 25 m and 45m, and antenna vertical beamwidths of 6˚ and 12˚. The simulation results of [6] determined within the range of typical microcellular the optimum downtilt angles were perceived to vary between 3.5˚ - 10.5˚ depending on the network configuration. In addition, the corresponding downlink capacity gain varied between 0-58%. The authors in [6] showed that the achievable capacity gain is higher with narrower antenna

vertical beamwidth. Also, with wider antenna vertical beamwidth, the selection of the downtilt angles becomes restricted.

The effect of BS antenna tilt on the performance of network Multiple Input Multiple Output (MIMO) antenna system with multi-antenna BSs was investigated in [7]. The study performed for a mobile network with inter-site distance of 500 m and BS antenna height of 32 m. The performance gains of MIMO networks over conventional systems critically depend on the selection of the right mechanical or electrical tilt angle. Mechanical tilt of the antenna refers to physically directing the antenna towards the ground, while electrical tilt is performed through adjusting the phases of antenna elements in an antenna array to downtilt the radiation pattern uniformly in the azimuth plane. The study of [7] showed that the electrical tilt angle outperforms the mechanical tilt angle. Furthermore, the performance of intra-site MIMO network performs almost the same as conventional system when the tilt angle is less than the optimum tilt angle. While both intra-site and inter-site MIMO networks perform identically if the tilt angles are larger than the optimum angle. The optimum electrical and mechanical tilt angle that provides the highest ASE, Cell-Edge UE throughput for conventional MIMO system is 14 degrees.

The impact of mechanical tilt and power control of the BS after shutting down idle BSs is studied in [8]. The study was performed for LTE-Advanced pico-cell system with a cell radius of 100 m at a carrier frequency of 2 GHz, and a BS antenna tilt angle between 0 degree and 20 degrees. The simulation results determined an optimum BS tilt angle of 15 degrees and showed that it is necessary to change BS antenna tilt and transmission power simultaneously to gain superior performance and energy efficiency.

A study is performed in [9] to investigate the impact of 3D base station antenna pattern on the performance of random heterogeneous cellular networks. A mathematical framework was proposed based on stochastic geometry and random shape theory to model BS location and building geometry, respectively, for both macro-cell and pico-cell BSs. The authors in [9] recommended to use relatively large vertical beamwidth for untilted BS antenna and smaller vertical beamwidth for down tilted BS antenna.

The function of tilt angle adaptation in LTE networks was investigated in [10] to reduce the interference using additional Single Input Multiple Output (SIMO) antenna system receivers and adaptive Orthogonal Frequency Division Multiplexing (OFDM) and Time Division Multiple Access (TDMA) transmission scheduling. They presented detailed performance measurements when (1) optimal fair tilt angle adjustment is applied in combination with SIMO receivers using Linear Minimum Mean Square Error (LMMSE) detection to attenuate interference and (2) when tilt angle adjustment is applied in combination with proportional fair OFDM transmission scheduling that adapts the transmission rate per subcarrier. It is found that using SIMO/LMMSE reception and adaptive transmission scheduling to mitigate interference, the adjustment of tilt angle led to improve the performance gain, namely an increase in mean user throughput of more than 65% and an improvement in the network sum-log rate of greater than 20%.

A self-optimization approach was proposed in [11] for mobile networks that obtain optimum capacity and coverage to improve network performance, while reducing operational costs and complexity. Results showed an improvement in the sum data rate of the network when enforcing antenna tilt angle optimization. Also, a self-optimization of the BS antenna electrical tilt is performed in [12]. The study in [12] considered dynamic and adaptive tilt

adjustment based on reinforcement learning methodology to perform a comparative analysis of several wireless propagation models on the downlink of a cellular network. The obtained simulation results showed that the accurate choice of channel model and related parameters is decisive to improve the performance of antenna tilt adjustment algorithm and the network.

A study performed in [13] to use conjugate beamforming with down tilted antennas for aerial UEs co-existence with multiple ground UEs. [13] investigated the impact of antenna downtilt angle, altitude, number of antennas, and number of scheduled UEs on the optimal performance. The results showed that the down-tilt angle of BS antennas can lead to tradeoff between the performance of the aerial UEs and the ground UEs when the altitude of the aerial UEs is below the BS antenna height.

The impact of the BS antenna downtilt on the performance of the downlink network in terms of the area spectrum efficiency and the coverage probability is investigated in [14]. The study analyzed the optimal antenna downtilt for a certain BS density considering 3D antenna pattern model. The results of [14] showed that the maximum coverage probability and significantly improved area spectral density, can be obtained for an optimal antenna downtilt.

The performance of LTE mobile network with antenna tilt is investigated in [15] to find the optimum parameter which impacts the Quality of Experience (QoE). A computationally efficient method for QoE-driven self-planning of antenna tilts is presented. Accordingly, the authors in [15] introduced new concepts of grouping cells into clusters without mutual interference to accelerate the search for the optimal solution with a classical gradient-based algorithm. The results showed a near-optimal solution for the overall system QoE with significantly low computational cost compared to other algorithms.

The authors of [16] studied the impact of the mechanical tilt angle of the BS on the performance of mm wave communication system at a carrier frequency of 28 GHz and an inter-site distance of 100 m. They studied the relationship between the performance and the tilting angle which can be led to mitigate the interference. Also, they proposed a general methodology to obtain the effective optimization of the tilt angle. Their results showed that the average SINR and the worst user SINR can be improved by using an optimal tilt angle. The optimal angle depends on several scenario-dependent parameters.

A study is performed in [17] to determine the impact of BS antenna tilt angle on the BS service provision of non-terrestrial network for Unmanned Aerial Vehicle (UAV) communication. The study focused on the two BS service provisioning schemes to support both ground UEs and aerial UEs with optimum antenna tilt angle design. The two BS service provisioning schemes are Inclusive-Service BS (IS-BS) and Exclusive-Service BS (ES-BS). The study derived the network outage probability for both schemes and analyzed the impact of the optimal tilt angles of different types of BS antennas on the outage probability. Moreover, they showed the impact of various network parameters on the performance of service provisioning schemes.

More recently, an additional set of uptilted cellular BS antenna were taken to serve drones and investigate the optimal uptilt angles in order to provide a reliable coverage at a drone corridor [18]. They identified five unique cases for aerial coverage that are dependent on the uptilt angles and beamwidths of the ground BS antennas. Moreover, the derived closed-form expressions for the signal-to-interference plus noise ratio (SINR) outage probability and the average SINR over a drone corridor. The results in [18] showed how the beamwidth and the maximum drone corridor height affect the optimal value of the antenna uptilt angle.

In [19], the authors proposed a novel cellular architecture that employs an extra set of antennas to provide reliable connectivity to the UAVs. Also, they proposed a modified path-loss model to catch the impact of the ground reflection (GR) on the UAVs. Moreover, an optimization of mathematical framework is proposed to maximize the minimum signal-to-interference ratio (SIR) of the UAVs by tuning the up-tilt (UT) angles of the up-tilted antennas.

The simulation results of [19] based on the hexagonal cell layout showed that the proposed interference attenuation method can ensure higher minimum SIRs for the UAVs over baseline methods while producing minimal impact on the SIR of ground user equipment (GUEs).

The impact of the BS antenna vertical pattern and downtilt on the downlink spatially averaged probability and area spectral efficiency (ASE) of a three dimensional (3D) two-tier Heterogenous cellular networks (HCNs) including macro-cell BSs (MBSs) and small-cell BSs (SBSs) is investigated in [20]. They derived the optimal BS antenna downtilt of both tiers that maximize the downlink spatially averaged coverage probability and ASE. The simulation results provided a good knowledge into the 3D deployment of BSs in HCNs.

The authors in [21] investigated the performance of cell-free multiple input multiple output systems serving ground user equipment (GUEs) and uncrewed aerial vehicles (UAVs) when varying the tilt angle of the access point antennas.

They studied the performance of antenna tilting employing two models: uniform linear arrays (ULA) and uniform planar arrays (UPA). They compared both models when serving both UAVs and GUEs in terms of mean user spectral efficiency (SE) and sum SE. The simulation results showed that when the uptilt benefits the UAVs, a fixed downwards antenna tilt angle (ATA) works better for the entire system. In addition, the UPA model works better for the system, while still prioritizing the GUEs in order to increase their SE.

As mentioned before, different studies were performed to investigate the impact of the BS antenna tilt angle on the performance of wireless cellular systems. However, none of the studies addressed the optimum BS tilt angle for different cell sizes, different BS antenna heights, and different carrier frequencies. Therefor The objectives of this paper are summarized as follows:

a) To study the effect of BS antenna tilt angle on the performance of LTE-Advanced system for different cell ranges, BS antenna heights, and carrier frequencies in realistic homogenous macro-cell scenarios. The cellular system is deployed with a frequency reuse factor of one that follows the 3rd Generation Partnership Project (3GPP) three-sector hexagonal grid. A site-specific ray tracing channel model is used to model the propagation channel of many BS–UE links. The study is performed for five cell ranges (250, 500, 750, 1000, 1250) m, two BS antenna heights (10, 30) m at carrier frequencies of 800 MHz and 2.6 GHz in (11 km x13 km) area in the city Centre of London, UK.
b) To determine the BS antenna tilt angle that maximizes the Average Spectrum Efficiency (ASE) or minimizes the UEs outage probability. Then determine a relation between these tilt angles and the tilt angles of the mean of SINR, rms delay spread, the received signal power, and received interference power.
c) To suggest optimum BS tilt angles for every cell range and BS antenna height that results in optimum ASE and outage probability.

The rest of the paper is organized as follows: Section 2 describes the system model including the channel model, cellular system layout and throughput estimation of the UEs.

Section 3 presents the simulation results of LTE-Advanced PDSCH for different BS tilt angles in terms of the mean of SINR, received average signal and interference power, rms delay spread, achievable THR, ASE, and UEs outage probability. Finally, conclusions are drawn in Section 4.

2. SYSTEM MODEL

2.1. Channel Model

This study uses Prophecy software to model the outdoor wireless channel of many BS-UE links. This program is developed at the University of Bristol in 1995 and validated by direct comparison with measurements at carrier frequencies ranging from 400 MHz to 2.6 GHz. The software performs ray tracing based on an urban site-specific database. The ray tracing engine models Multi Path Components (MPCs) through identifying all possible direct, reflected, refracted, and scattered ray paths between the transmitter and the receiver in 3D space. The database includes terrain, buildings, and foliage. The available database is for two urban environments in the United Kingdom. The first is a 4 km × 4.4 km area in central Bristol and the second is an 11 km × 13 km area in central London [22].

A previous study performed by an author of this paper in [23] validated the Inter-Site Interference (ISI) results obtained from the ray tracing tool using ISI measurements previously reported for London in [24]. The validation study in [23] compared the received interference power at of many individual interfering BS-UE links in terms of the CDF and median of the Dominant Interference Proportion (DIP). The Ray Tracing Channel Model (RTCM) is deterministic model and preferred over the standardized Geometry based Stochastic Channel Model (GSCM) of the International Telecommunication Union (Radio communication sector (ITU-R for the following reasons[23]:

- Simplified angle spread distributions are assumed in the GSCMs [25].
- A wide range of frequencies are defined in the GSCMs for distribution functions used for random processes, while some parameters are frequency dependent. For example, the decorrelation distance of the Root Mean Square (RMS) delay spread reported in the ITU-R channel model [25] for LoS UE locations in urban macro scenario is 30 m over the frequency range from 450 MHz to 6 GHz. However, our previous work in [26] based on ray tracing modelling at carrier frequencies of 800 MHz and 2.6 GHz showed the decorrelation distance is dependent on frequency.
- The 3D ray model is map based and can be applied to study a wide range of realistic site-specific deployments.

2.2. Cellular System Layout

The layout of the mobile communication system is based on a homogenous macro-cell cellular deployment with a frequency reuse factor of one and 3GPP hexagonal cells. As shown in Fig. 1(a), each hexagon cell represents a sector. Each BS site consists of three sectors with a radius R and a cell range of 2R. The inter site distance between the cells is 3R [27]. The serving BS site lies at the center with ICI caused by nine interfering cells that belong to the first tier of six interfering BS sites surrounding the serving BS site. The ray tracer was used to predict the MPCs for the serving BS-UE and interfering BS-UE channels at many BS and UE locations to

provide statistical representative results. Within the ray tracer 18 macro cellular BSs were placed on rooftop locations in the city center of London in the United Kingdom. Many UEs were randomly scattered at street level within each cell of the serving BS site. The number of UE locations in each cell for each scenario is presented in Table 1. The study is performed for different BS tilt angles considering different cell ranges and BS antenna heights at carrier frequencies of 800 MHz and 2.6 GHz. The macro BS and UE antenna patterns shown in Fig. 1(b, and c) are used in this study. Patterns were obtained from anechoic chamber measurements performed at the University of Bristol [28]. All patterns were captured in 3D and include phase, polarization and directivity information. The BS antenna pattern in Fig.1(b) is for a tilt angle of 10 degrees. The same antenna patterns are assumed and used for both frequency bands. The BS transmit powers for different cell ranges are taken from [29] and validated in [30]. Equal transmit power are assumed for both carrier frequencies based on [31]. Table 1summarizes the system parameters used in this paper.

Table 1. System model parameters.

Parameter		Value				
LTE advanced bandwidth [MHz]		10				
No. of subcarrier (N_{SC})		600				
No. of OFDM symbols		7				
T_{slot} [ms]		0.5				
Carrier frequency		800 MHz, 2.6 GHz				
Environments		11 km × 13 km area in central London				
Cellular deployment		3GPP, 3-sector, hexagonal grid, reuse factor of 1				
BS antenna height [m]		10, 30				
BS antenna tilt angle [degree]		2 to 44 in steps of 2				
Minimum BS_UE distance [m]		50				
Cell range [m]		250	500	750	1000	1250
BS transmit power [W]		2	5	10	20	40
No. of UEs per sector		180	290	385	440	490
No. of BS		12				
BS antenna down-tilt		2° to 50° in steps of 2°				
UE sensitivity [dBm]		-120				
Used antennas		Macro-BS			UE	
Antenna height [m]		10, 30			1.5	
Directivity gain [dBi]		13.2			6.5	
Antenna type		Uniform linear array of 6 dual polarized patch antennas			(Omni-directional) like antenna from a NOKIA mobile	
Antenna beamwidth	azimuth	65°			360°	
	elevation	15°			36°	
Antenna system		Single antenna system				

The SINR at each user location, u, within the serving BS site, S, and the interfering BS sites, ($I: I_1, I_2, \ldots I_6$), is given by Eq. (1):

$$SINR_u^S = \frac{P_u^S}{P_{AWGN} + \sum_{ICI} P_u^I} \quad (1)$$

In Eq. (1), P_u^S and P_u^I represent the average received power at location u associated with the serving BS sector cell and the interfering cells, respectively. The average received power at a UE location, u, is obtained from the summation of the received power of the predicted rays (MPCs). The interference power is gathered across all interferers. The Additive White Gaussian Noise (AWGN) power, P_{AWGN}, in watt is calculated using Eq. (2):

$$P_{AWGN} = \mathcal{K} \times T_K \times B_N \times F \quad (2)$$

In Eq. (2), $\mathcal{K}$ is Boltzmann's constant, T_K is the noise temperature in Kelvin, B_N is the effective noise bandwidth in Hz, and F is the noise figure (linear value). The effective noise bandwidth, B_N, represents the product of the number of subcarriers (N_{SC}) and the subcarrier spacing (Δf) of the OFDM system. In this study, a 10 MHz LTE-Advanced bandwidth is assumed along with $T_K = 288°$ *Kelvin* (15°C), Δf =15 kHz, and $F_{dB} = 9$ dB [27].

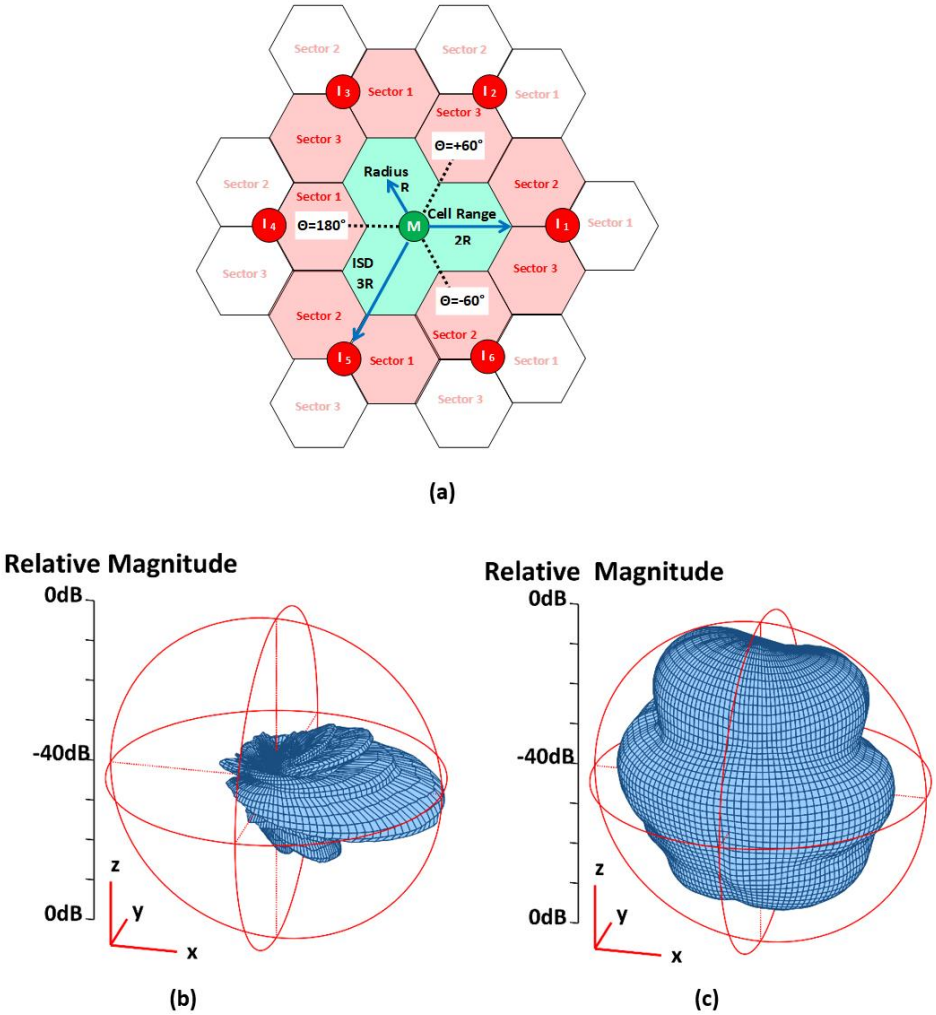

Fig. 1. The network layout and the total power radiation patterns of the BS and UE antennas: a) 3GPP - 3 sector hexagonal grid deployment with a frequency reuse factor of one; b) macro BS antenna [28]; c) UE antenna [28]

2.3. Throughput Estimation of the UEs

The work presented in this paper is a system-level simulation study which includes many BS locations, many BS-UE links, two carrier frequencies, two environments, five cell ranges, twenty-five BS antenna tilt angles (see Table 1), and different Modulation and Coding Schemes

(MCS) (see Table 2). These studies are time consuming when performed using bit accurate physical layer simulators. However, the Received Bit mutual Information Rate (RBIR) technique can be used as a computational efficient alternative to bit level simulation when studying the system level performance of OFDM based communication system [32]. The validation study of [33], performed by an author of this paper, shows an excellent agreement between bit level simulation and RBIR abstraction results. The RBIR runs around 300 times faster on the same computing platform.

The channel impulse response for each serving BS-UE link is generated using the 3D ray tracer, converted into the frequency domain, and used as the input into our Physical Downlink Shared Channel (PDSCH) RBIR simulator to estimate the instantaneous Packet Error Rate (PER) for 10 MCS modes at the average SINR determined by Eq. (1). The information required in Eq. (1) and Eq. (2) are also obtained from 3D ray tracing of the serving BS-UE links and the interfering BS-UE links. A link adaptation algorithm is applied to select the MCS that maximizes the throughput (*THR*) of each link. The *THR* of LTE-Advanced PDSCH for a specific MCS (THR_{MCS}) is calculated using Eq. (3) [34] as a function of the peak error free data rate (R_{MCS}) and the *PER* for the considered MCS mode.

$$THR_{MCS} = R_{MCS}\,(1 - PER_{MCS}) \tag{3}$$

For a single antenna system, R_{MCS} can be calculated using Eq. (4) in terms of the number of modulation order (k_m), the coding rate (R_C), the number of active subcarriers (N_{SC}), and the number of OFDM symbols (N_{SYM}) in a time slot (T_{slot}). Table 1 summarizes the system parameters used here, while Table 2 lists the value of R_{MCS} for each considered MCS mode.

$$R_{MCS} = \frac{k_m \cdot R_C \cdot N_{SC} \cdot N_{SYM}}{T_{slot}} \tag{4}$$

The achievable THR (THR_A) at the UE locations is determined using Eq. (5) from the MCS mode that produces the highest THR.

$$THR_A = \max\{THR_1, THR_2, \ldots\ldots, THR_{10}\} \tag{5}$$

Table 2. List of MCS modes and peak error free data rates.

MCS	Modulation	Code rate	R_{MCS} [Mbps]
1	QPSK (k_m=2)	1/3	5.6
2		1/2	8.4
3		2/3	11.2
4		4/5	13..44
5	16QAM (k_m=4)	1/2	16.8
6		2/3	22.4
7		4/5	26.88
8	64QAM (k_m=6)	2/3	33.6
9		3/4	37.8
10		4/5	40.32

3. RESULTS AND ANALYSIS

This section shows the simulation results of LTE-Advanced PDSCH for different BS tilt angles considering a single antenna system and following the 3GPP hexagonal cellular

deployment with a frequency reuse factor of one. The study is performed for cell ranges of (250, 500, 750, 1000, 1250) m and BS antenna heights of (10, 30) m using a site-specific 3D ray tracing channel model in the city center of London at carrier frequency of 800 MHz and 2.6 GHz. The results are presented and compared in terms of SINR, received average signal and interference power, rms delay spread, achievable THR, Average Spectrum Efficiency (ASE), and UE outage probability.

3.1. Channel Model Parameter and Achievable Throughput

This section shows the Cumulative Distribution Function (CDF) graphs of the received average signal power, received total ICI power, and the rms Delay Spread (DS) for different cell range and carrier frequencies at a reference BS tilt angle of 10 degrees. The conclusion and discussion made in this section may apply for a tilt angle of 10 degrees only. Analyzing the results at other BS tilt angles might lead to different conclusion. The selection of a tilt angle of 10 degrees is based on the BS tilt angle of the current deployed macro cellular systems [35]. The results are obtained from the ray tracing data for many BS and UE locations as listed in Table 1.

Fig. 2(a) shows CDF graphs of the received average signal power for different cell ranges and two carrier frequencies. As expected, the 800 MHz band provides higher received signal power compared to the 2.6 GHz band. This is due to the higher pathloss of the 2.6 GHz band compared to the 800 MHz band.

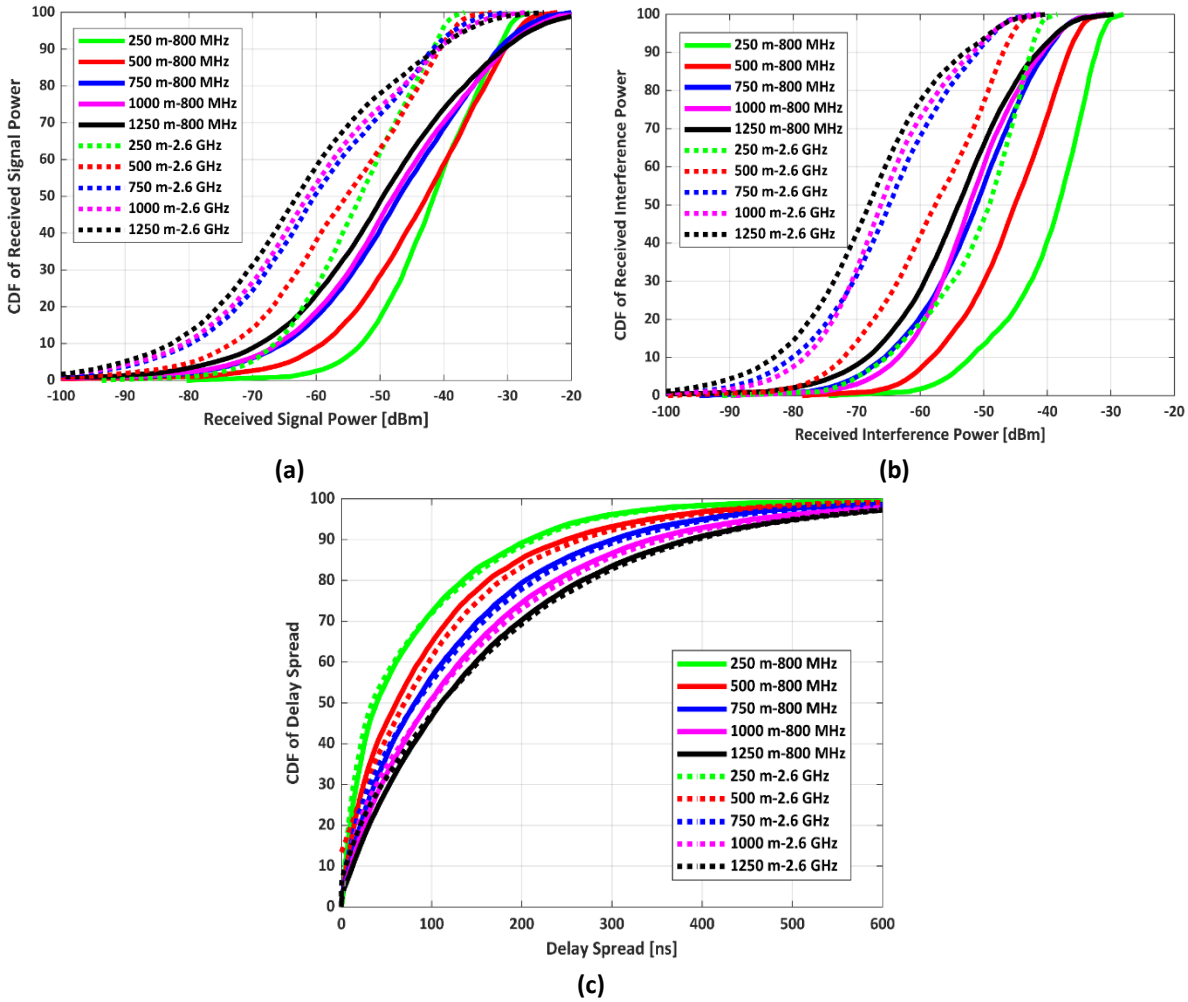

Fig. 2. Channel characteristic for different cell ranges and carrier frequencies (BS antenna height =30 m, BS antenna tilt angle =10 degree): a) received signal power; b) received total interference power; c) RMS delay spread.

Fig. 2(a) also shows two regions for the received signal power. The first region is the high received power region that belongs to UE locations close to the serving BS. In this region, relatively higher received power is observed for the larger cell ranges. This is because of the higher transmit power of the larger cell ranges (see Table 1) combined with the relatively lower pathloss of the UE locations near the BS. The second region is the low received power region. In this region the received power decreases as the cell range increases despite the higher transmit power of the larger cell ranges. The attenuation in the received signal strength due to the increase in the cell range is dominant.

The CDF graphs of the received total interference power are shown in Fig. 2(b). The received total interference power decreases as the cell range increases and the carrier frequency increases. As the cell range increases, the distance between the interfering BS and the UEs in the serving BS site increases. This increase in the distance and the increase in the carrier frequency led to a higher pathloss for the interfering BS-UE links. Fig. 2(c) shows the CDF graphs of the rms DS for different cell ranges and carrier frequencies. It is clear from the graphs that the rms DS is nearly the same for both frequency bands since the rms DS is independent of the carrier frequency [36, 37]. However, the figure shows that the rms DS increases as the cell range increase. This is because the propagated signal suffers higher dispersion due to multipath effect as the cell range increases.

Fig. 3 shows the CDF of the SINR and the achievable throughput for many UE locations for a reference BS tilt angle of 10 degrees. Fig. 3(a) shows two regions, high SINR region and low SINR region. In the high SINR region, higher SINR levels are observed as the carrier frequency increases and the cell range increases. This is due to the reduction of the received total interference power when the cell range and the carrier frequency increase as shown in Fig. 2(b). Although increasing the cell range and carrier frequency leads to decrease in the received signal strength too, the reduction in the total interference is dominant. Consequently, the achievable throughput at the UE locations increases as the cell range and the carrier frequency increase as shown in Fig. 3(b).

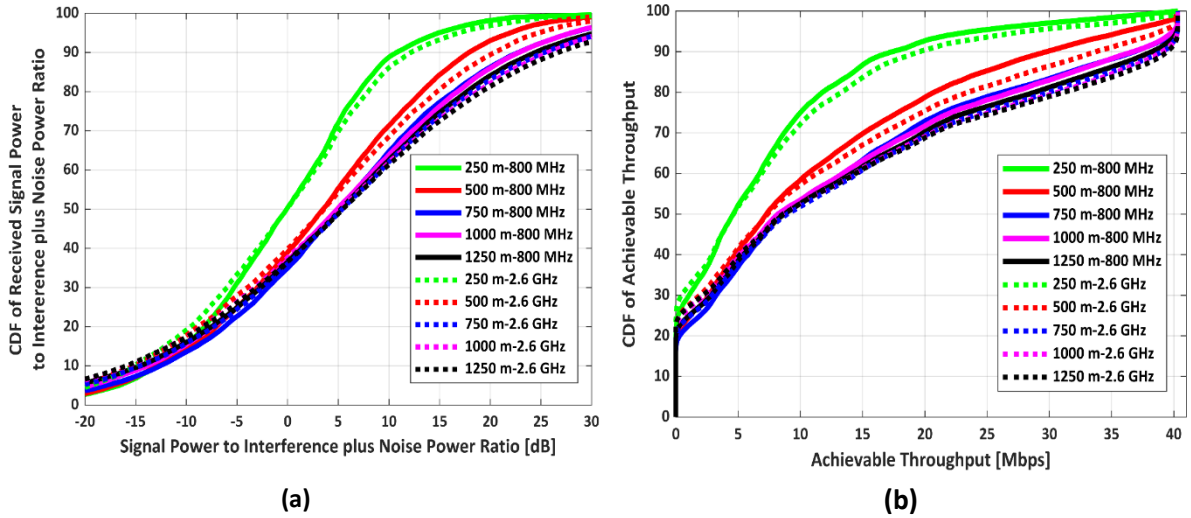

Fig. 3. CDF of SINR and achievable throughput for different cell ranges and carrier frequencies (BS antenna height =30 m, BS antenna tilt angle =10 degrees): a) SINR; b) achievable throughput.

3.2. Impact of BS Tilt Angles on ASE

This section investigates the impact of BS tilt angle on the ASE for different cell ranges, different BS antenna heights, and different carrier frequencies. The study is conducted for cell

ranges of 250 m, 500 m, 750 m, 1000 m, and 1250 m considering BS antenna heights of 10 m and 30 m. The BS tilt angles are changed from 2 degrees to 44 degrees in steps of 2 degrees. The analysis also considers the impact of the BS tilt angle on other channel parameters such as SINR, rms DS, received signal power, and received interference power. The ASE is measured in bit/second/Hz/Cell (bps/Hz/Cell) and defined as the aggregate throughput for all users normalized by the overall cell bandwidth and the number of cells [38]. Also, the term (maximum ASE tilt) is used here to refer to the BS tilt angle that provides maximum ASE.

Fig. 4 shows the performance of ASE, SINR, rms DS versus BS tilt angle for different carrier frequencies, different BS antenna heights, and a cell range of 250 m. The data tips marked on the figures shows the related parameter for a conventional BS tilt angle of 10 degrees as a reference.

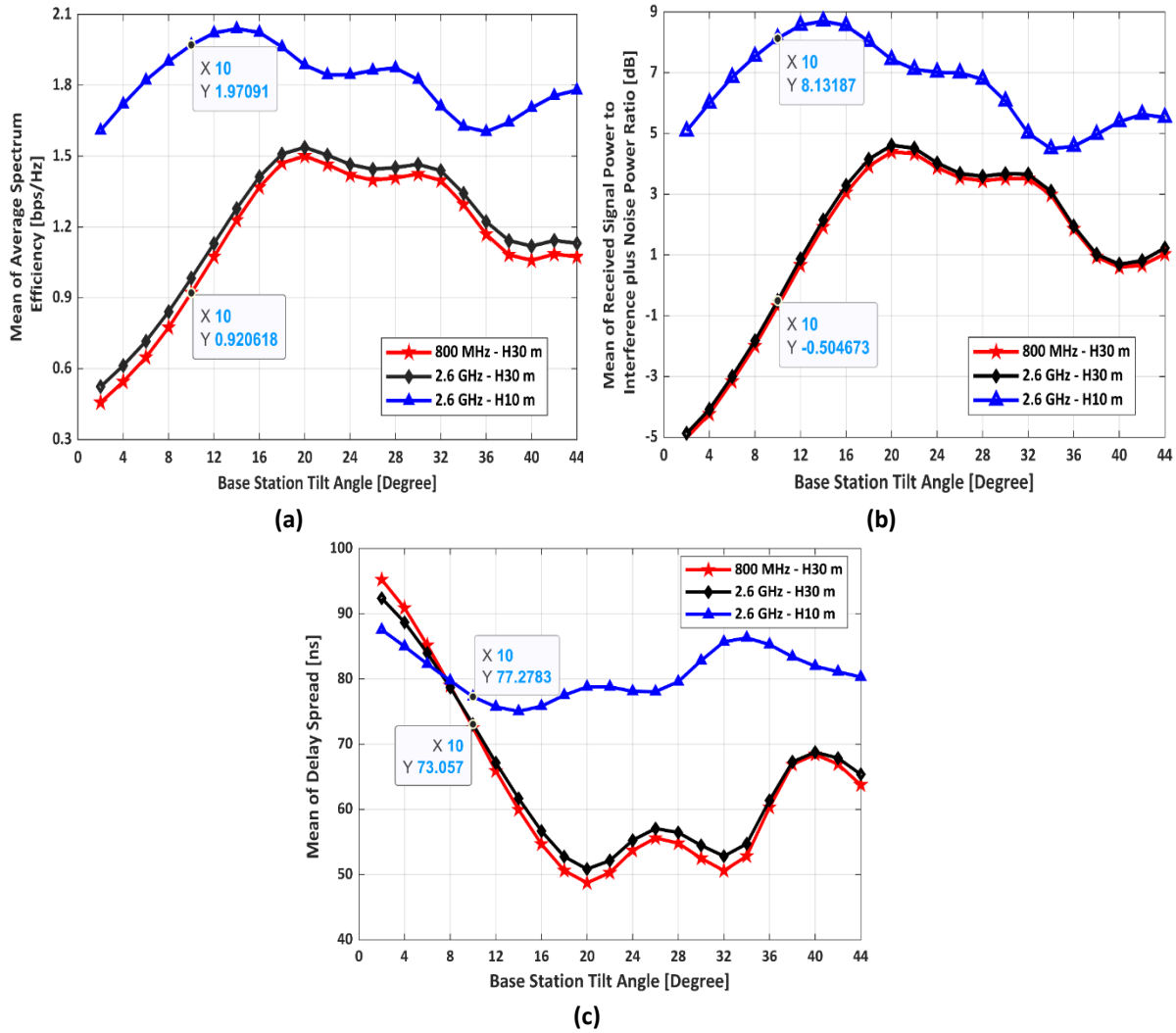

Fig. 4. BS tilt angle for different BS antenna heights and carrier frequencies with a cell range of 250 m versus: a) ASE; b) SINR; c) delay spread.

It is clear from Fig. 4(a) that the maximum ASE occurs at a BS antenna tilt angle of 20 degrees at both carrier frequencies when the BS antenna height is 30 m. The maximum ASE tilt angle decreases to 14 degrees as we decrease the BS antenna height to 10 m. Comparing the ASE at the maximum ASE tilt angle and a conventional BS tilt angle of 10 degrees, maximum ASE tilt angles of 20 degrees and 14 degrees provides improvements in the ASE by factors of

1.63 and 1.03 for BS antenna heights of 30 m and 10 m, respectively. The improvement is significant for the 30 m BS antenna height compared to the 10 m. From Fig. 4(b, and c), for an antenna height of 10 m and a BS tilt angle of 10 degrees, the SINR and rms DS are 8.13 dB and 77.28 ns, respectively. These values change to 8.70 dB and 75.03 ns when the BS tilt angle increased to 14 degrees. The difference in the SINR and the rms DS between the conventional and the best ASE tilt angles for the 10 m BS antenna height are 0.67 dB and -2.25 ns, respectively. These differences are small, leading to a small increase in the ASE. For a BS antenna height of 30 m, these differences in the SINR and the rms DS between the conventional and the best ASE tilt angle increase to 5.11 dB and -22.21 ns. It is obvious that these differences lead to a significant increase in the ASE.The ASE is calculated from the achievable THR at the UE locations which in turn are functions of the PER. The SINR and the rms DS are two parameters of the wireless channel that determines the PER, THR, and ASE performance. Fig.4(b) and Fig. 4(c) show the mean value of the SINR (in dB) and rms DS (in ns) for different BS tilt angles. It is clear from the two figures that the highest SINR and lowest rms DS occur at a maximum ASE tilt angle. These results justify and confirm the results of Fig. 4(a). Compared to a BS tilt angle of 10 degrees, Fig. 4(b) shows around 5.1 dB improvement in the mean of the SINR at the maximum ASE tilt for BS antenna height of 30 m and 0.57 dB improvement in the case of BS antenna height of 10 m. Similarly, the maximum ASE tilt angle results in minimum mean of the rms DS at the maximum ASE tilt angles. The reduction factor in the mean of the rms DS for BS antenna height of 30 m and 10 m are around 1.5 and 1.03, respectively.

Comparing the ASE graphs of Fig. 4(a) in terms of carrier frequency and BS antenna height, both frequency bands provide nearly the same ASE performance for the same BS antenna height. This is because both frequency bands provide approximately the same mean of SINR and rms DS for the same BS antenna height. In contrast, for the same carrier frequency, as the BS antenna height decrease from 30 m to 10 m, the SINR level increases leading to increase in the ASE. As shown in Fig. 4(c), decreasing the BS antenna height from 30 m to 10 m results also in increase in the mean of the rms DS too. But the increase in the SINR is dominant and has more impact in increasing the achievable THR and the ASE.

The relation between the rms DS and the BS antenna height is different for different environments. In the macro cellular environment, such as the one considered in this study, the BS antenna is located at height higher than the obstacles between the BS and the UE links [39]. In such scenarios the probability of LoS UE locations increase as the BS antenna increases. As the probability of LoS increases, the mean of the rms DS decreases. The results shown in Fig. 4(c) confirm this fact. For example, at BS tilt angle of 10 degrees, the means of the rms DS decreased from 77.28 ns to 73.06 as the BS antenna height increased from 10 m to 30 m. This is because the probability of LoS UE locations increased from 29% for 10 m BS antenna height to 45.71% for BS antenna height of 30 m.

In contrast, the study performed in [40] for micro cellular systems shows that the mean of the rms DS increase as the BS antenna height increased from 3.7 m to 13.3 m. This is because in micro cellular scenario, the BS antenna is located typically at the same height as lampposts in a street and often at a similar height on the side of a building. The change in the antenna height does not affect the probability of LoS. The mean of the rms DS are affected by the pathloss of the BS-UE links for different heights where the pathloss increased as the BS antenna height increased from 3.7 m to 13.3 m.

To justify the performance of the mean SINR versus BS tilt angle of Fig. 4(b), Fig. 5 shows the impact of BS tilt angle on the mean values of received signal power and the received total interference power for BS antenna height of 30 m at a carrier frequency of 800 MHz and a cell range of 250 m. As the tilt angle increases, the received signal power increases till a tilt angle of 16 degrees, then the received signal power starts to decrease as the tilt angle increases beyond 16 degrees. In the same way, the received total interference power increases first till the tilt angle reaches 10 degrees, then it starts to decay as the tilt angle increases. The difference between the received signal power (in dBm) and the received total interference power (in dBm) varies as the tilt angle increases. As indicated by the green arrow, maximum difference occurs at a BS tilt angle of 20 degrees. This value represents the maximum ASE tilt angle where the ASE and the SINR are maximum.

In Fig. 5, maximum received power occurs at a BS tilt angle of 16 degrees which is different from the maximum ASE tilt angle. However, at this tilt angle the difference between the received signal power and received interference power (in dBm value) is not maximum. The maximum difference between the received signal power and received total interference power can be observed at the maximum ASE tilt angle of 20 degrees as indicated by the green arrow in Fig. 5.

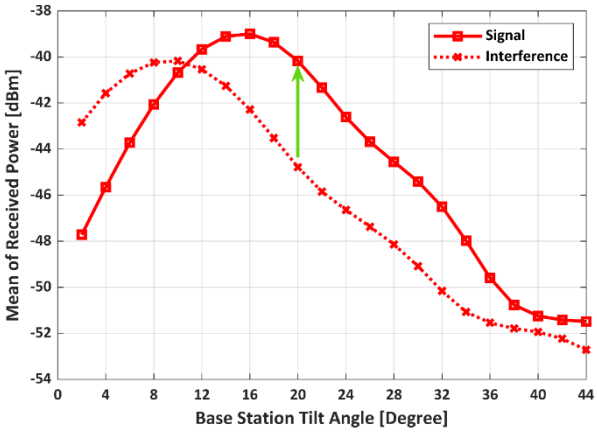

Fig. 5. Received signal and interference power versus BS tilt angle (BS antenna heights=30 m, carrier frequency=800 MHz, cell range = 250 m).

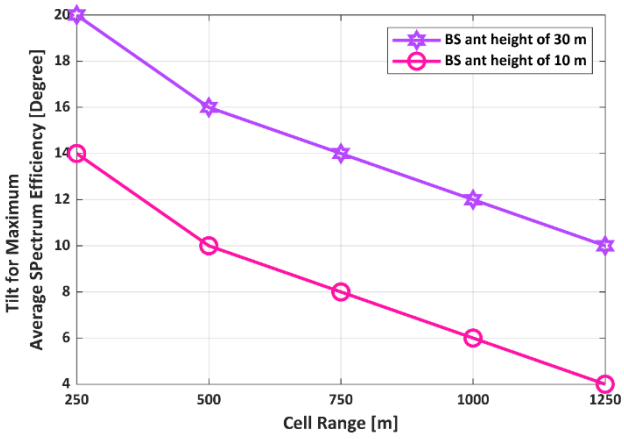

Fig. 6. Maximum ASE BS tilt angle versus cell range for different BS antenna heights.

Following the same above procedure, Fig. 6 shows the maximum ASE tilt angle for different cell ranges. It is worth mentioning that these tilt angles apply for both frequency bands as concluded from Fig. 4. It is obvious from Fig. 6 that for all the considered cell ranges, the

maximum ASE tilt angle of a BS antenna height of 10 m is 6 degrees less than the maximum ASE tilt of BS antenna height of 30 m.

3.3. Impact of BS Tilt Angle on UEs Outage Probability

This section studies the effect of BS antenna tilt angle on the UEs outage probability for different cell ranges, different BS antenna heights, and different carrier frequencies. A UE is in outage if its achievable THR drops to zero [38]. Also, the term (minimum outage tilt) is used here to refer to the BS tilt angle that provides minimum probability of UEs outage. Fig. 7 shows the UEs outage probability and the mean of the received signal power versus BS tilt angle for different BS antenna heights and different frequency bands for a cell range of 250 m. The data tips marked on the figures shows the related parameter for a conventional BS tilt angle of 10 degrees as a reference. As shown in Fig. 7(a), the mean of outage probability of the UEs changes as the BS tilt angle changes. The best (minimum) outage tilt occurs at a BS tilt angle of 16 degrees for both frequency bands when the BS antenna height is 30 m. This angle represents the BS tilt angle where the mean of the received signal power is maximum as shown in Fig. 7(b). Like the maximum ASE tilt, the minimum outage tilt decreases to 10 degrees when the BS antenna height is decreased to 10 m. At this angle the received signal power is maximum. Therefore, the minimum outage tilt angle represents the BS tilt angle that maximizes the received signal power.

Comparing the outage probability for a BS antenna height of 30 m in Fig. 7(a) in terms of the carrier frequency, the 800 MHz band experience lower outage probability than the 2.6 GHz band for all the tilt angles. As shown in Fig. 7(b), this is because the mean of received signal power of the 800 MHz band is higher compared to the 2.6 GHz band. The difference in the mean of the received power is around 11.6 dB for all tilt angles. This is because the only difference between these two scenarios is the carrier frequency. Fig. 7(b) also shows that the mean of the received power increase as the BS antenna height increase. This is because the probability of LoS UE location increases from 29% to 45.71% when the BS antenna height increases from 10 m to 30 m. Increasing the BS antenna height in macro cellular system leads to increase in the the probability of LoS UE locations. Since LoS UE location experience higher received signal power, this in turn leads to increase in the mean of the received signal power and as the BS antenna height increase in macro cellular systems [30].

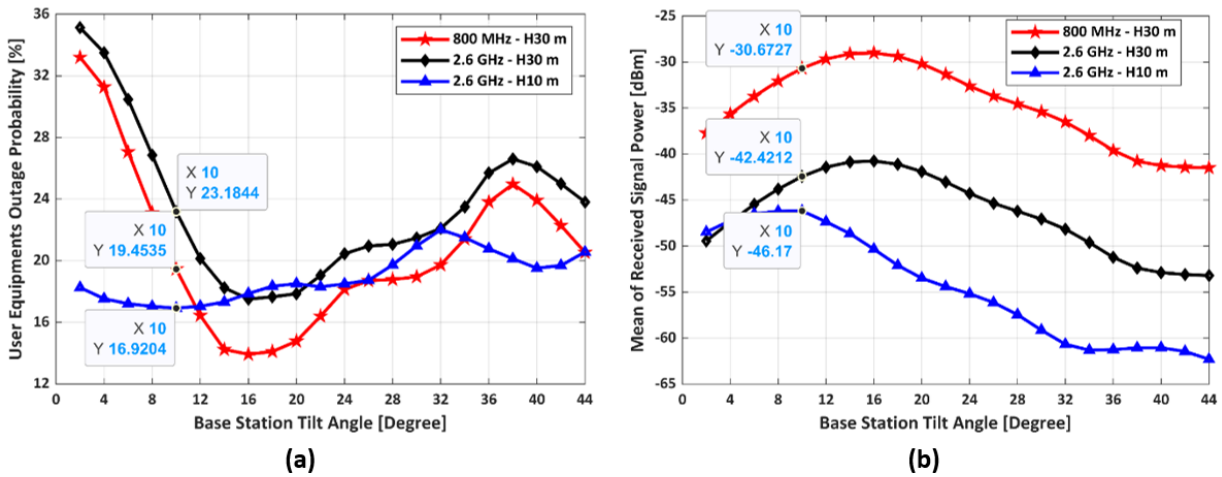

Fig. 7. UEs outage probability and received signal power versus BS tilt angle for different BS antenna heights and carrier frequencies with a cell range of 250 m: a) probability y of UEs outage; b) mean of received signal power.

Fig. 8 shows the tilt angles and the mean of the received signal power for minimum outage probability for different cell ranges and BS antenna heights in the 2.6 GHz band. Similar to the maximum ASE tilt angles, the minimum outage tilt angle in Fig.8(a) decrease as the cell range increases and the BS antenna height decreases. This is applicable at both frequency bands. For the cell ranges of 250 m, 500 m, and 1000 m, the difference between the minimum outage tilt for BS antenna height of 30 m and 10 m is equal to 6 degrees, which is like the maximum ASE tilt case. But this difference is 8 degrees and 4 degrees for cell ranges of 750 m and 1250 m.

It is clear from Fig. 8(b) that mean of the received signal power decrease as the BS antenna height decreases and the cell range increases. For both BS antenna height, the difference in the mean received signal power for cell range of 750 m and above is small. For a BS antenna height of 30 m, the received signal power is higher and more sensitive to the tilt angle compared to the received power of the 10 m BS antenna height. The mean of the received signal power for a BS antenna height of 10 m and a cell range of 750 and above varies between -73 dBm and -75 dBm. This signal strength is very low compared to the signal strength and less sensitive to BS tilt angle. Thus, the tilt angle and the mean of the received signal power for minimum outage probability decreases as the cell size increase and BS antenna height decrease. But, and determined in [6], the large cell ranges (750 and above) has less impact on the minimum outage tilt angle.

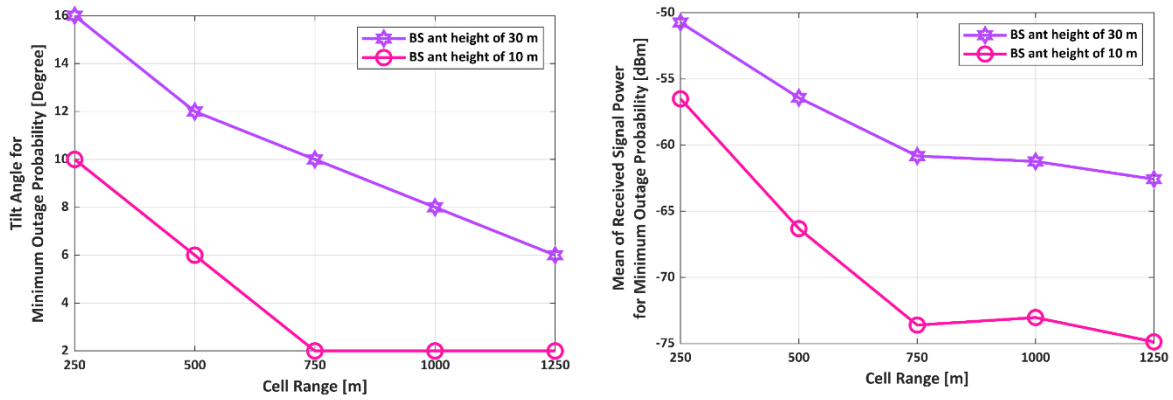

Fig. 8. BS tilt angle and mean of received signal power for minimum outage versus cell range for different BS antenna heights at a carrier frequency of 2.6 GHz: a) BS tilt angle; b) mean of received signal power.

3.4. Optimum BS Tilt Angles

This section looks at the maximum ASE and the minimum outage tilt angles and suggests optimum BS tilt angles accordingly. Comparing Fig. 6 and Fig. 8(a), it can be noticed that the minimum outage tilt angles are different and smaller than the maximum ASE tilt angles. When the BS antenna height is 30 m, the difference between the maximum ASE tilt angles and the minimum outage tilt angles are 4 degrees for all cell ranges. The same difference applies for a BS antenna height of 10 m, except for the cell ranges of 750 m and 1250 m where the differences are 6 degree and 2 degrees, respectively. Optimum tilt angles can be selected between the minimum outage tilt and the maximum ASE tilt to provide optimum ASE and outage probability.

For example, for a BS antenna height of 30 m and a cell range of 250 m at the 800 MHz band, the maximum ASE tilt angle is 20 degrees (see Fig. 6), and the minimum outage tilt angle is 16 degrees (see Fig. 8). If the tilt angle is selected to be 20 degrees when deploying the BS

antenna of the cellular system, the ASE is maximum, but the outage probability increases from 13.9% to 14.8% of the UEs as shown in Fig. 7(a). The outage probability increases by 0.9% compared to the minimum outage. In the same way, if the 16 degree is chosen to be the tilt angle of the BS antenna, the outage probability remains minimum, but the ASE decreases by 0.13 bps/Hz from 1.5 bps/Hz to 1.37 bps/Hz (see Fig. 4(a)). However, if an optimum tilt angle of 18 degrees is selected, the reduction in the ASE and the increase in the outage probability will be less resulting in an optimum ASE and outage probability. The 18 degrees in this case represents the midpoint between 16 and 20 degrees. Now, the reduction in the ASE is 0.03 instead of 0.13 bps/Hz and the increase in the outage probability is 0.18% instead of 0.9%.

Table 3 lists the suggested optimum BS tilt angle along with maximum ASE and minimum outage probability tilt angles. As determined from Fig 4(a) and Fug.7(a), this table is applicable for both frequency bands, the 800 MHz and the 2.6 GHz.

The optimum BS tilt angles of recommended in this paper for different BS antenna height and cell ranges in LTE-Advanced system are close to the optimum BS tilt angles obtained in the literature for comparable scenarios. The study performed in [6] for CDMA system recommended optimum angles of 8.1 degrees and 7.5 degrees for site separations of 1.5 km and 2 km, respectively, when the BS antenna height is 35 m. These scenarios are comparable to cell ranges of 1000 m and 1250 m and BS antenna height of 30 m. In our scenarios the optimum angles are 10 degrees and 8 degrees, respectively. The difference in the values is small and are due the difference in the BS antenna height and the algorithm used for determining the optimum angle of two different wireless systems. The study in [4] performed for CDMA system with a site separation of 1.5 km recommended a tilt angle of 12 degrees. While our results in Table 3 recommends an optimum BS tilt angle of 10 degree for a cell range of 1000 m. The recommended BS tilt angle of [4] is 2 degrees larger compared to our case. The BS antenna height in [4] was 40 m and in our study was 30 m, thus the tilt angle is larger [6]. where the BS antenna height is 30 m. Also, the study [8] recommended an optimum BS tilt angle of 15 degrees for LTE-Advanced pico-cell with a cell radius of 100 m. Our paper recommends a BS tilt angle of 12 degrees for macrocell with a cell range of 250 m and BS antenna height of 10 m. This difference belongs to the difference in the cell size where the optimum tilt angle s as the cell range increases [6]. Fig. 9 shows CDF graphs of the achievable THR at a carrier frequency of 800 MHz for a BS antenna height of 30 m. Fig. 9(a) shows CDF graph of the achievable THR for different cell ranges considering the optimum BS tilt angles in Table 3. Unlike the results of Fig. 3(b) which are obtained for a BS tilt angle of 10 degrees, selecting the optimum BS tilt angle for each cell range results in approximately the same CDF of the achievable THR.

Table 3. BS antenna tilt angles for best and optimum ASE and Outage probability for the 800 MHz and 2.6 GHz bands.

Cell Diameter [m]	BS antenna tilt angle [degrees]					
	Max ASE		Min Outage		Optimum	
	H10	H30	H10	H30	H10	H30
250	14	20	10	16	12	18
500	10	16	6	12	8	14
750	8	14	2	10	5	12
1000	6	12	2	8	4	10
1250	4	10	2	6	3	8

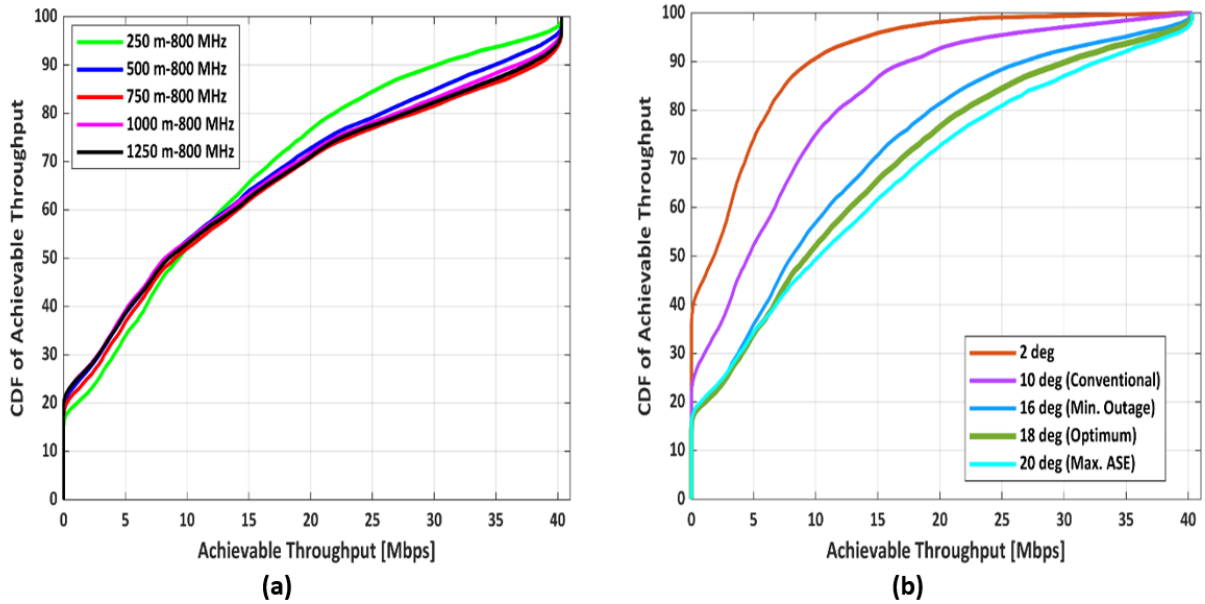

Fig. 9. CDF of achievable throughput for different cell ranges and BS antenna tilt angle (BS antenna height=30m, carrier frequency 800 MHz): a) optimum BS tilt angle; b) selected tilt angle with a cell range of 250 m.

Fig. 9(b) shows the impact of the BS tilt angle on the achievable THR with a cell range of 250 m for selected BS antenna tilt angles of (2, 10, 16, 18, 20) degrees. The 10 degrees represent the BS antenna tilt angle in conventional macro-cell mobile cellular system [35]. The angles (16, 18, 20) represent the minimum outage, optimum, and maximum ASE tilt angles that are selected from Table 3 based on the results.

It is clear from the CDF graphs that the achievable THR increases as the BS antenna tilt angle increases from 2 degrees to 20 degrees. For example, when BS tilt angle is 2 degrees, the achievable THR of around 90% of the UEs are smaller than 10 Mbps.

The percentage of UEs that experience an achievable THR less than or equal to 10 Mbps decreases to around 75%, 57%, 53%, and 50% when the BS antenna tilt angles are 10, 16, 18, and 20 degrees, respectively. This means as the BS tilt angle increases up to the maximum ASE tilt angle, more UEs experience achievable THR greater than 10 Mbps.

Also, it can be noticed that the CDF graphs of the achievable for the optimum tilt angle (green line), maximum ASE tilt angle (cyan line), and minimum outage tilt angle (blue line) are close to each other.

Finally, Fig. 10 shows the coverage map of the achievable THR for a BS site for a cell range of 250 m and a BS antenna height of 30 m at a carrier frequency of 800 MHz considering the selected tilt angles of Fig. 9(b). The red circle in the middle of the coverage maps represents the location of the BS. Also, no UEs are observed near the BS location because the minimum BS-UE distance is set to 50 m in this study as listed in Table 1.

It is clear from the coverage maps how the achievable THR at different UE locations increases as the BS antenna tilt angle increases. The blue color (THR between 0 and 15 Mbps) is dominant in both Fig. 10(a) and Fig. 10(b) for BS antenna tilt angles of 2 and 10 degrees, respectively.

The UE locations with green and yellow colors (from 20 to 40 Mbps) increase when the BS antenna tilt angle changes to minimum outage, optimum, and maximum ASE tilt angles as shown in Fig. 10 (c, d, and e).

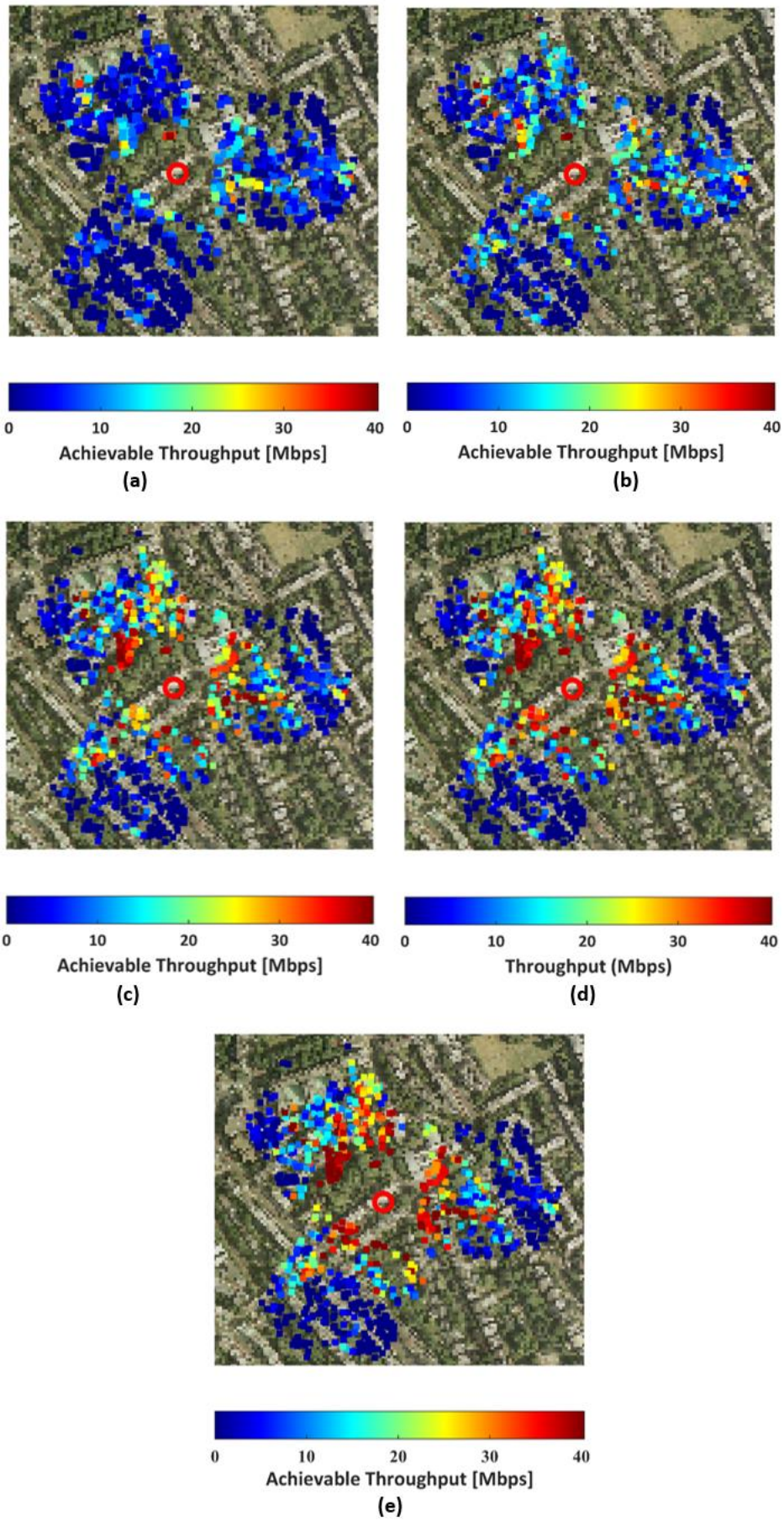

Fig. 10. Coverage map of the achievable THR in London (cell ranges 250 m, carrier frequency 800 MHz, BS antenna height 30 m) for BS tilt angles: a) 2 degrees; b) 10 degrees; c) 16 degrees; d) 18 degrees; e) 20 degrees.

4. CONCLUSIONS

This paper investigated the impact of BS antenna tilt angle on the performance of physical downlink shared channel of the LTE-Advanced system. The study was performed for a single antenna system through a system level simulation for many BSs and UE links considering hexagonal 3GPP homogenous deployment with a frequency reuse factor of one. The multipath wireless communication channel between the main BS-UE links and the interfering BS-UE links for many BSs and UE locations are modelled using an urban site-specific 3D ray tracing tool in the city center of London, UK for BS with cell ranges of (250, 500, 750, 1000, 1250) m and BS antenna heights of (10, 30) m at carrier frequencies of 800 MHz and 2.6 GHz. An RBIR abstraction model was used to the PER and determine the achievable THR, ASE, and UEs outage probability.

The system level study was performed for many BS antenna tilt angles between 2 and 44 degrees in steps of 2 degrees. The results were used to determine the tilt angle that provides the maximum ASE or the minimum UEs outage probability. The following conclusions are drawn:

- Both the maximum ASE and the minimum outage BS tilt angles decrease as the cell range increases and the BS antenna height decreases. But they are independent of carrier frequency.
- At the maximum ASE BS antenna tilt, the mean of the SINR is maximum and the mean of the rms delay spread is minimum. Therefore, SINR and rms delay spread can be used instead of ASE to determine the maximum ASE tilt angle.
- At the minimum outage BS antenna tilt, the mean of the received signal power is maximum. Hence, the received signal power can be used instead of outage probability to determine the maximum ASE tilt angle.
- A difference of six degrees was observed between the best BS tilt angles when the BS antenna height is 30 m compared to the 10 m. Also, the difference between maximum ASE tilt angle and minimum outage tilt angle is 4 degrees for most cases.
- Based on the results, a list of optimum BS tilt angles was suggested to provide optimum ASE and outage probabilities.

REFERENCES

[1] Z. Chen, K. Luk, *Antennas for Base Stations in Wireless Communications*, New York: McGraw-Hill, 2009.

[2] Y. Zhou, L. Liu, H. Du, L. Tian, X. Wang, J. Shi, "An overview on intercell interference management in mobile cellular networks: From 2G to 5G," IEEE International Conference on Communication Systems, 2014, doi**:** 10.1109/ICCS.2014.7024797

[3] E. Benner, "Effects of antenna height, antenna gain, and pattern downtilting for cellular mobile radio, " *IEEE Transaction on Vehicular Technology*, vol. 45, no. 2, pp. 217–224, 1996, doi: 10.1109/25.492845.

[4] J. Niemela, J. Lempiainen, "Impact of mechanical antenna downtilt on performance of WCDMA cellular network," 59th Vehicular Technology Conference, 2004, doi: 10.1109/VETECS.2004.1390642.

[5] S. Khan, P. Lahdekorpi, J. Lempiainen, "Impact of repeaters and base station antenna tilt on performance of a WCDMA macro cellular network for different network topologies," 19th Telecommunications Forum Proceedings of Papers, 2011, doi: 10.1109/TELFOR.2011.6143558.

[6] J. Niemelä, T. Isotalo, J. Lempiäinen, "Optimum antenna downtilt angles for macrocellular wcdma network," *Journal on Wireless Communications and Networking*, vol. 5, pp. 816-827, 2005, doi:10.1155/WCN.2005.816.

[7] N. Seifi, M. Coldrey, M. Matthaiou, M. Viberg, "Impact of base station antenna tilt on the performance of network MIMO systems," 75th Vehicular Technology Conference, 2012, doi: 10.1109/VETECS.2012.6239994.

[8] Y. Gao, Y. Li, S. Zhou, Y. Li, H. Yu, "System level performance of energy efficient dynamic mechanical antenna tilt angle switching in LTE-Advanced systems," IEEE International Wireless Symposium, 2013, doi: 10.1109/IEEE-IWS.2013.6616832.

[9] X. Li, T. Bai, R. Heath, "Impact of 3D base station antenna in random heterogeneous cellular networks," Wireless Communications and Networking Conference, 2014, doi: 10.1109/WCNC.2014.6952680.

[10] B. Partov, D. Leith, R. Razavi, "Tilt angle adaptation in LTE networks with advanced interference mitigation," 25th Annual International Symposium on Personal, Indoor, and Mobile Radio Communication, 2014, doi: 10.1109/PIMRC.2014.7136492.

[11] N. Dandanov, H. Al-Shatri, A. Klein, V. Poulkov, "Dynamic self-optimization of the antenna tilt for best trade-off between coverage and capacity in mobile networks," *Wireless Personal Communications*, vol. 92, pp. 251–278, 2017, doi: 10.1007/s11277-016-3849-9.

[12] N. Dandanov, S. Samal, S. Bandopadhaya, V. Poulkov, K. Tonchev, P. Koleva, "Comparison of wireless channels for antenna tilt based coverage and capacity optimization," Global Wireless Summit, 2018, doi: 10.1109/GWS.2018.8686597.

[13] R. Amer, W. Saad, N. Marchetti, "Toward a connected sky: performance of beamforming with down-tilted antennas for ground and UAV user co-existence," *IEEE Communications Letters*, vol. 23, no. 10, pp. 1840-1844, 2019, doi: 10.1109/LCOMM.2019.2927452.

[14] J. Yang, M. Ding, G. Mao, Z. Lin, D. Zhang, T. Luan, "Optimal base station antenna downtilt in downlink cellular networks," *IEEE Transactions on Wireless Communications*, vol. 18, no. 3, pp. 1779-1791, 2019, doi: 10.1109/TWC.2019.2897296.

[15] P. Ordóñez, S. Ramírez, M. Toril, "A computationally efficient method for QoE-driven self-planning of antenna tilts in a LTE network," *IEEE Access*, vol. 8, pp. 197005-197016, 2020, doi: 10.1109/ACCESS.2020.3033325.

[16] M. Rebato, L. Rose, M. Zorzi, "Tilt angle optimization in dynamic TDD mmwave cellular scenarios," *IEEE Communications Letters*, vol. 24, no. 11, pp. 2637-2641, 2020, doi: 10.1109/LCOMM.2020.3008870.

[17] S. Kim, M. Kim, J. Ryu, J. Lee, T. Quek, "Non-terrestrial networks for UAVs: base station service provisioning schemes with antenna tilt," *IEEE Access*, vol. 10, pp. 41537-41550, 2022, doi: 10.1109/ACCESS.2022.3166241.

[18] S. Maeng, M. Chowdhury, İ. Güvenç, A. Bhuyan, H. Dai, "Base station antenna uptilt optimization for cellular-connected drone corridors," *IEEE Transactions on Aerospace and Electronic Systems*, vol. 59, no. 4, pp. 4729-4737, 2023, doi: 10.1109/TAES.2023.3237994.

[19] M. Chowdhury, İ. Guvenç, W. Saad, A. Bhuyan, "Ensuring reliable connectivity to cellular-connected UAVs with up-tilted antennas and interference coordination," *ITU Journal on Future and Evolving Technologies*, vol.2, pp. 165-185, 2021, doi: 10.48550/arXiv.2108.05090.

[20] M. Zhou, C. Chen, X. Chu, "Impact of 3D antenna radiation pattern on heterogeneous cellular networks," *IEEE Access*, vol. 10, pp. 120866-120879, 2022, doi: 10.1109/ACCESS.2022.3223089.

[21] M. Lobão, W. Feitosa, R. Antonioli, Y. Silva, W. Jr, G. Fodor, "On the impact of antenna tilt on cell-free systems serving ground users and UAVs," XLI Brazilian symposium on telecommunications and signal processing , 2023, doi: 10.14209/sbrt.2023.1570917523.

[22] E. Tameh, A. Nix, "The use of measurement data to analyse the performance of rooftop diffraction and foliage loss algorithms in a 3-D integrated urban/rural propagation model," 48th IEEE Vehicular Technology Conference, 1998, doi: 10.1109/VETEC.1998.686584.

[23] A. Ameen, A. Doufexi, A. Nix, "Proposed ITU-R compatible inter-site and inter-sector interference models for LTE-advanced networks," *IEEE Transactions on Vehicular Technology*, vol. 69, no. 12, pp. 14304-14315, 2020, doi: 10.1109/TVT.2020.3044952.

[24] *3GPP R4-061281*, 2006, www.3gpp.org.

[25] *ITU-R M.2135-1,* 2009, www.itu.int.

[26] R. Almesaeed, A. Ameen, E. Mellios, A. Doufexi, A. Nix, "A proposed 3D extension to the 3GPP/ITU channel model for 800 MHz and 2.6 GHz bands," 8th European Conference on Antennas and Propagation, 2014, doi: 10.1109/EuCAP.2014.6902468.

[27] *3GPP TS36.942*, 2010. <www.3gpp.org>

[28] E. Mellios, Z. Mansor, G. Hilton, A. Nix, J. McGeehan, "Impact of antenna pattern and handset rotation on macro-cell and pico-cell propagation in heterogeneous LTE networks," Proceedings of the IEEE International Symposium on Antennas and Propagation, 2012, doi:10.1109/APS.2012.6348849.

[29] FUJITSU Network Communications, "High-Capacity Indoor Wireless Solutions: Picocell or Femtocell? ", 2013, www.fujitsu.com/us/Images/High-Capacity-Indoor-Wireless.pdf.

[30] A. Ameen, D. Berraki, A. Doufexi, A. Nix, "LTE-advanced network inter-cell interference analysis and mitigation using 3D analogue beamforming," *IET Communications*, vol. 12, no. 13, pp. 1563-1572, 2018, doi: 10.1049/iet-com.2017.0765.

[31] H. Shajaiah, A. Abdelhadi, T. Clancy, "Towards an application-aware resource scheduling with carrier aggregation in cellular systems," *IEEE Communications Letters*, vol. 20, no. 1, pp. 129-132, 2016, doi: 10.1109/LCOMM.2015.2495294.

[32] 3GPP TSG-RAN-1 Meeting #35, R1-03-1298: "Effective SIR computation for OFDM system-level simulations," 2003, www.3gpp.org.

[33] A. Ameen, E. Mellios, A. Doufexi, N. Dahnoun, A. Nix, "LTE-advanced downlink throughput evaluation in the 3G and TV white space bands," 24th Annual International Symposium on Personal, Indoor, and Mobile Radio Communications, 2013, doi: 10.1109/PIMRC.2013.6666240.

[34] K. Beh, A. Doufexi, S. Armour, "Performance evaluation of hybrid ARQ schemes of 3GPP LTE OFDMA system," 18th International Symposium on Personal, Indoor and Mobile Radio Communications, 2007, doi: 10.1109/PIMRC.2007.4394852.

[35] R. Aquino, S. Zaidi, D. McLernon, M. Ghogho, A. Imran, "Tilt angle optimization in two-tier cellular networks—a stochastic geometry approach," *IEEE Transactions on Communications*, vol. 63, no. 12, pp. 5162-5177, 2015, doi: 10.1109/TCOMM.2015.2485981.

[36] A. Ameen, E. Mellios, A. Doufexi, N. Dahnoun, A. Nix, "LTE-advanced downlink throughput evaluation in the 3G and TV white space bands," *Annual International Symposium on Personal, Indoor, and Mobile Radio Communications*, 2013, doi: 10.1109/PIMRC.2013.6666240.

[37] M. Steer, "Antennas and the RF link," *Microwave and RF Design I - Radio Systems*, North Carolina State University, 2019, https://eng.libretexts.org/@go/page/41163.

[38] 3GPP TR36.913, "Requirements for Further Advancements for Evolved Universal Terrestrial Radio Access; (LTE Advanced-Release10),"2011, www.3gpp.org.

[39] S. Saunders, A. Zavala, *Antenna and Propagation for Wireless Communication Systems,* John Wiley & Sons, 2007.

[40] M. Feuerstein, K. Blackard, T. Rappaport, S. Seidel, H. Xia, "Path loss, delay spread, and outage models as functions of antenna height for microcellular system design," *IEEE Transactions on Vehicular Technology,* vol. 43, no. 3, pp. 487-498, 1994, doi: 10.1109/25.312809.